

Optical absorption properties of Ag/SiO₂ composite films induced by gamma irradiation

This article has been downloaded from IOPscience. Please scroll down to see the full text article.

2003 J. Phys.: Condens. Matter 15 9

(<http://iopscience.iop.org/0953-8984/15/2/302>)

View [the table of contents for this issue](#), or go to the [journal homepage](#) for more

Download details:

IP Address: 171.66.16.119

The article was downloaded on 19/05/2010 at 06:26

Please note that [terms and conditions apply](#).

Optical absorption properties of Ag/SiO₂ composite films induced by gamma irradiation

A L Pan^{1,2,4}, H G Zheng³, Z P Yang³, F X Liu^{1,2}, Z J Ding^{1,2} and Y T Qian³

¹ Structure Research Laboratory, University of Science and Technology of China, Hefei, Anhui 230026, People's Republic of China

² Department of Astronomy and Applied Physics, University of Science and Technology of China, Hefei, Anhui 230026, People's Republic of China

³ Department of Chemistry, University of Science and Technology of China, Hefei, Anhui 230026, People's Republic of China

E-mail: pananlian@sina.com

Received 17 July 2002, in final form 30 October 2002

Published 20 December 2002

Online at stacks.iop.org/JPhysCM/15/9

Abstract

Mesoporous SiO₂ composite films with small Ag particles or clusters dispersed in them were prepared by a new method: first the matrix SiO₂ films were prepared by the sol–gel process combined with the dip-coating technique; then they were soaked in AgNO₃ solutions; this was followed by irradiation with γ -rays at room temperature and ambient pressure. The structure of these films was examined by high-resolution transmission electron microscopy, and their optical absorption spectra were examined. It has been shown that the Ag particles grown within the porous SiO₂ films are very small and are highly dispersed. On increasing the soaking concentration and subjecting the samples to an additional annealing, a different peak-shift effect for the surface plasmon resonance was observed in the optical absorption measurement. Possible mechanisms of this behaviour are discussed in this paper.

1. Introduction

Nanometre-sized ultrafine metal and semiconductor particles display many intriguing properties, including optical nonlinearity [1], specific heat [2], and magnetism properties [3] which are quantitatively and qualitatively different from those of the respective bulk materials. In the past decade, much attention has been paid to the study of composites of nanometre particles embedded in various matrices, from the viewpoints of scientific interest [4, 5] and applications [6–9]. Mesoporous SiO₂ made by the sol–gel method, with interconnected nanoscale pores and high specific surface area, has recently been used as a new exotic kind

⁴ Author to whom any correspondence should be addressed.

of matrix for metal/semiconductor-nanoparticle-doped materials. Recently Cai and Zhang [8] have successfully assembled mesoporous silica with Ag nanoparticles within its pores by the thermal decomposition method and found an optical switching phenomenon to be exhibited by the optical absorption edge with increasing metal particle size. Tomokatsu and his team have incorporated Ag particles in a Eu-doped SiO₂ matrix by the H₂ reduction route, and found a remarkable enhancement effect of Ag particles on the fluorescence of Eu³⁺ in a SiO₂ matrix [9]. In addition, in studying composites doped with nanometre metal particles, many people taken an interest in the surface plasmon resonance (SPR) peaks of these ultrafine particles because of their changeable properties and potential applications. Palpant and co-workers [10] investigated the surface plasmon energy ($w_{surf} = w_p/[1 + \text{Re } \epsilon_d(w_{surf})]^{1/2}$) of silver clusters in the framework of the time-dependent local density approximation (TDLDA), and proved theoretically that the size evolution of Mie frequency ($w_m = w_p/[2 + \text{Re } \epsilon_d(w_m)]^{1/2}$) is very sensitive to the matrix and the porosity at the interface, and it is similar to the surface plasmon frequency. $w_p = [3q^2/4\pi r_s^3 \epsilon_0 m]^{1/2}$ is the free-electron plasma frequency, and $\epsilon_d(w)$ is the core electron contribution to the complex dielectric function of the metal $\epsilon(w)$. r_s is the Wigner–Seitz radius of the bulk metal. Gamma irradiation has been used extensively to generate novel nanomaterials with unusual properties starting from a few years ago [11–13], since it can help in preparing materials at room temperature and ambient pressure, and it is easily controlled and adaptable, and cannot induce impurities in the matrix. Recently, we have combined γ -irradiation with the well-known sol–gel process and dip-coating technique, and successfully developed a new method for synthesizing silver-nanoparticle-doped mesoporous SiO₂ films; we found a different peak-shift effect for the optical absorption band (SPR) for these films. In this paper, we will give a simple discussion of their alterable optical absorption character.

2. Experimental details

The silver-doped SiO₂ composite films were prepared by a new and simple method at room temperature and ambient pressure. First of all, analytical grade tetraethoxysilane (TEOS, 98%), alcohol, HNO₃, and deionized water were mixed together in the molar ratios 1:7:1:10. The mixture was stirred magnetically until it became a homogeneous solution, which would serve for dip-coating. Then the mesoporous silica films were obtained by dipping 1 mm thick substrate glass into the dip-coating solution, and subsequently dried and aged in a sealed box with several pinholes in the top cover at 60 °C. Then the glasses with sol–gel films on both sides were slowly heated to 650 °C for 2 h in an oven to expel residual solvent from the pores, and then the porous SiO₂ substrate films were prepared. Second, several pieces of the pre-formed porous SiO₂ films were soaked in AgNO₃ solutions of different concentrations at room temperature for several weeks. After immersion, the soaked SiO₂ films together with the soaking solution were irradiated by a ⁶⁰Co γ -ray source (2.59×10^{15} Bq) for 4 h to expel the silver (from the AgNO₃) out of the pores. Then, the irradiated samples were taken out of the soaking solutions and washed with distilled water, then dried at 80 °C in a vacuum dryer. To study the effect of heat on our samples, the as-prepared composite films were additionally annealed at 350, 550, and 750 °C in Ar gas for 2 h. The preparation conditions are shown in table 1. The Ag/SiO₂ films obtained were blue or purple in colour and quite transparent enough for use in optical studies.

Direct observations of the morphology and the lattice fringe of the Ag particles were performed using a JEOL 2010 high-resolution transmission electron microscope (HRTEM). The optical absorption spectra were measured using a UV-365 recording spectrophotometer in the range from 300 to 700 nm at room temperature. The chemical states of the Ag particles in the pre-formed composite films were analysed by x-ray photoelectron spectroscopy using a Mg K α x-ray source.

Table 1. Preparation conditions and corresponding particle size and SPR peak position. (The irradiating dose was 15 674 Gy.)

Sample	Soaking concentration (M)	Annealing temperature (°C)	Particle size (nm)	Peak position (nm)
1	0.01	80	0.9 (1.0) ^a	370
		350	1.7	392
		550	2.3	425
		750	3.9	405
2	0.05	80	1.8 (2.0) ^a	414
		350	3.2	424
		550	4.0	407
		750	5.0	400
3	0.5	80	4.0 (4.3) ^a	421
		350	4.8	405
		550	5.5	396
		750	6.2	393

^a Mean diameter from HRTEM examination.

3. Results and discussion

Figure 1 shows the HRTEM morphology micrographs for the SiO₂ films soaked in 0.01, 0.05, and 0.5 M AgNO₃ solutions and irradiated with γ -rays for 4 h (samples 1–3, dried at 80 °C). The top right images are a selected-area electron diffraction pattern and a lattice fringe image for particles dispersed in sample 2. The morphology micrographs show nearly spherical particles highly uniformly dispersed in the films. The mean particle sizes in each of the films determined by measuring the sizes of 50 particles in an enlarged morphology micrograph are 1.0, 2.0, and 4.3 nm respectively. The values of interplanar spacing d_{hkl} calculated from the diameters of the diffraction rings agree with those of bulk silver. There are no other crystallites (including AgNO₃) to be found in our examination. Therefore, it is reasonably concluded that the microcrystallites dispersed in the pores of mesoporous SiO₂ films were all silver particles.

Figure 2 shows the optical absorption spectra of our samples. Curve (a) is for the substrate glass, curve (b) is for the Ag-doped porous SiO₂ films soaked in 0.01 M AgNO₃ and dried at 80 °C, but curves (c)–(e) are for sample (b) subjected to subsequent additional annealing at 350, 550, and 750 °C for 2 h, respectively. Curve (a) does not show any peak in the range of 300–700 nm. But the curve for the silver-doped sample exhibits a band or peak around 400 nm which is due to the SPR absorption peak or band of Ag particles or clusters [14]. With increasing annealing temperature, the SPR peak for the Ag particles exhibited a significant shift accompanying the narrowing and increase in intensity of the spectra, which indicates growth of the Ag particles dispersed in the porous film. Using the relation [15]

$$r = V_F / \Delta w_{1/2}$$

(where $\Delta w_{1/2}$ is the full width at half-maximum (FWHM) of the SPR band in the angular frequency, r is the average particle radius, and V_F is the Fermi velocity of an electron and is 1.39×10^6 m s⁻¹ for silver), the mean particle diameters of the Ag particles in our samples were evaluated and are also shown in table 1. From the table, we know that the particle size calculated is slightly smaller than that measured directly through HRTEM and that both are good fits. Figure 3 shows the annealing temperature dependences of the peak position and the mean silver diameter. With increasing annealing temperature, the silver particles dispersed in the films become bigger and bigger, which indicates that the Ag has a relatively high mobility in

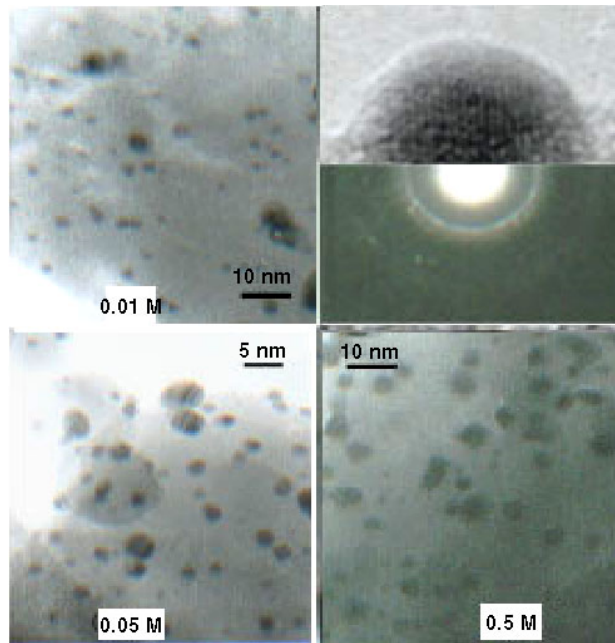


Figure 1. HRTEM morphology micrographs for the SiO₂ films soaked in 0.01, 0.05, and 0.5 M AgNO₃ solutions and irradiated with γ -rays for 4 h (samples 1–3, as originally formed). The top right images are a selected-area electron diffraction pattern and a lattice fringe image for particles dispersed in sample 2.

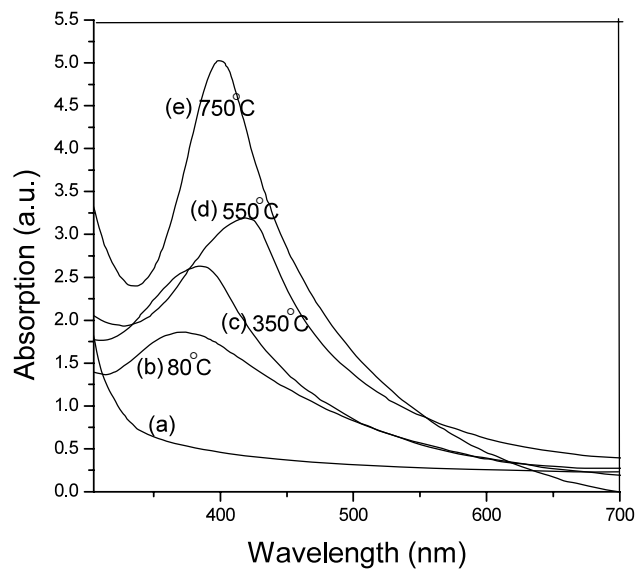


Figure 2. Optical absorption spectra for the substrate glass (a), and the Ag-doped porous SiO₂ film dried at 80 °C (b), as well as the corresponding additionally annealed samples (b)–(d).

our films. The observed cluster growth can be explained by an aggregation mechanism similar to Ostwald ripening, in which larger particles grow at the expense of smaller ones during the cooling of the sample [16]. For samples soaked in different concentrations of AgNO₃ solution,

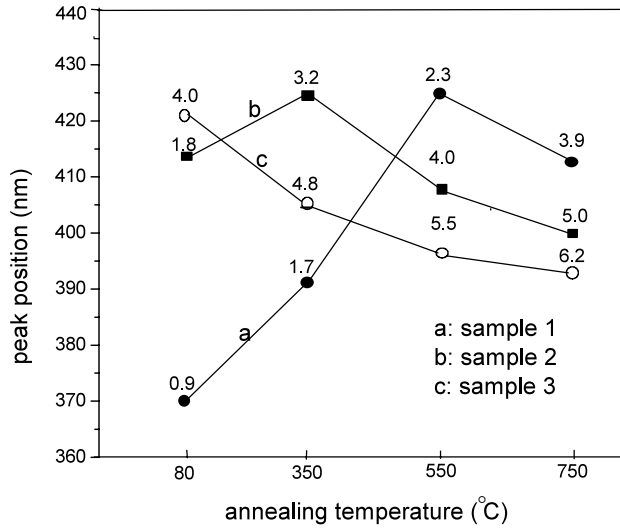


Figure 3. The annealing temperature dependences of the peak position and the mean silver diameter for the SiO₂ films soaked in 0.01 M (a), 0.05 M (b), and 0.5 M (c) AgNO₃ solution and irradiated with γ -rays for 4 h. The value near each symbol shows the mean particle size for the corresponding sample. The solid lines are just guides for the eye.

the peak-shift directions are different: the ones soaked in 0.01 or 0.05 M AgNO₃ show a red-shift at first, then change to showing a blue-shift with increasing annealing temperature, but the ones immersed in 0.5 M AgNO₃ only exhibit a blue-shift (or a red-shift with decreasing particle size).

It is well known that the position of the SPR peak for small free Ag particles will blue-shift with decreasing particle size (the size effect), which can be explained by the Mie and relevant Mie-like theories [10, 14, 17, 18] and the energy band theory [19]. Since the peak-shift direction of our sample is different from that for free Ag particles, the influence of the matrix may play an important role. In our Ag/SiO₂ systems, the Ag nanoparticles are not free but are uniformly dispersed within pores of the mesoporous SiO₂ matrix, which has a high specific surface area and great porosity [20], and a large number of dangling bonds (unsaturated bonds) exist on the pore walls, probably resulting in high surface energy and chemical activity [17, 21, 22]. Also, in the case of small particles, the extension of the electronic wavefunction outside the ion core becomes significant [23]. Thus the dangling bonds on the pore walls are likely to accommodate electrons transferred from the Ag particles at the interface in order to relax the interface energy and reach a more stable state. These interactions at the interfaces between the pore walls and the Ag particles, through the coupling of electrons transferred from the Ag particles, can induce a decrease of the free electron density in the Ag particles and the SPR frequency will thus be decreased (i.e., show a red-shift) according to relation [14]

$$\omega_s \approx (n_e e / \varepsilon_0 m_{eff})^{1/2} (2\varepsilon_{matrix} + 1 + \chi_{1,interband})^{-1/2}$$

where n_e , e , m_{eff} are the density, charge, and effective mass of the conduction electrons respectively, ε_0 and ε_{matrix} are the dielectric constant in vacuum and the actual dielectric constant of the matrix material, and $\chi_{1,interband}$ is the real part of the interband transition susceptibility. Further, these interactions will probably become more prominent with decreasing Ag particle size because of the increased activity of the electrons on the small particle surface, and can probably lead to a large red-shift of the resonance band.

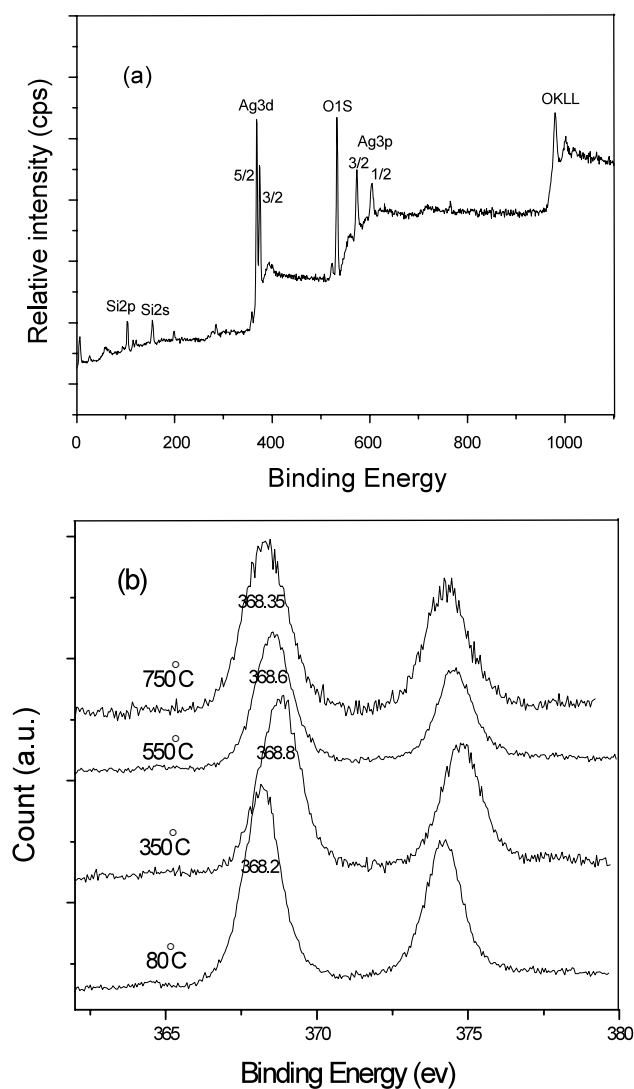


Figure 4. (a) is the XP spectrum of the sample immersed in 0.01 M AgNO_3 but without additional annealing (sample 1 dried at 80°C). (b) shows the XP spectra of Ag 3d for sample 1 as originally formed and the ones additionally annealed at different temperatures.

In order to confirm the influence of the matrix, we investigated the x-ray photoelectron (XP) spectra of the sample. Figure 4(a) shows the XP spectrum of the sample immersed in 0.01 M AgNO_3 without additional annealing (sample 1 dried at 80°C). As shown in figure 4(a), in all XP spectra of the measured samples, almost no elements other than silver, oxygen, and silicon were detected. The peak position for Ag $3d_{3/2}$ shown in figure 4(a) is 368.20 eV, which is the binding energy of bulk silver. This means that the very small Ag clusters are just adsorbed physically on the pore walls of the SiO_2 matrix and the interactions between the particles and the matrix are very weak. When the dispersed clusters are too small compared to the pore size, they could be more like free clusters because of the large porosity at the cluster/matrix interface [10]. Figure 4(b) shows the XP spectra of Ag 3d for sample 1 as

originally formed and the ones additionally annealed at different temperatures. It shows that the binding energy of the Ag 3d shifts to the higher-energy side with additional heat treatment, indicating the existence of an interaction between the Ag particles and the matrix. However, with the annealing temperature increasing from 350 to 750 °C, the binding energy is gradually decreased. The decrease of the binding energy with increase of the annealing temperature indicates increasing of the s–d screening interaction in the surface region of the particles, which we think is just a result of the decreasing number of free electrons transferred from the Ag particles to the surrounding SiO₂ matrix with increasing particle size.

Thus the size evolution of the Mie frequency of our embedded Ag particles should be a net result of the competition between the intrinsic size effect and the extrinsic influence of the surrounding medium. It is reported that the intrinsic quantum size effects of small free Ag clusters are prominent when the size is below ~2 nm [24, 25]. As shown in figure 3, when the dispersed particles are too small compared to the pore sizes, they are more like free clusters, and the intrinsic quantum size effect is more prominent than the influence from interactions between the clusters and the pore walls; only an intrinsic blue-shift effect for the SPR band is exhibited with decreasing particle size (see curves (a), (b)). In contrast, as the dispersed particles become bigger and bigger, resulting in a smaller and smaller porosity at the interface, the dispersed particles cease to be seen as free clusters [10]. At the same time, the finite quantum size effect will quickly decrease with increasing particle size. The interactions between the clusters and the pore walls will eventually dominate, and a red-shift of the SPR band will be exhibited with decreasing particle size, as discussed above. Depending on the sizes of the particles dispersed in the pre-formed sample, the additional annealing can induce both a red-shift and a blue-shift (curves (a), (b)) or just a blue-shift (curve (c)) of the peak with increasing treatment temperature.

4. Conclusions

In summary, we have successfully synthesized Ag-nanoparticle-doped porous SiO₂ films by a new γ -radiation method. The Ag particles are isolated and highly dispersed, and the particle size was easily controlled. With increasing annealing temperature, a significant red-shift of the SPR absorption peak for the Ag particles dispersed in samples 1 and 2 was exhibited at first; this was interpreted in terms of the better-known size effect. But a higher-temperature annealing of samples 1 and 2 and an additional annealing of the pre-annealed sample 3 induced a blue-shift of the resonance peak instead; this was explained as the result of stronger interactions between Ag particles and the matrix.

Acknowledgments

This work was supported in part by the National Natural Science Foundation of China (Nos 10025420, 20075026), the Foundation of Chinese Education Committee and the Key Foundation of USTC.

References

- [1] Uchida K, Kaneko S, Omi S, Hata C, Tanji H, Asahara Y, Ikushima A J, Tokizaki T and Nakamura A J 1994 *J. Opt. Soc. Am. B* **11** 1236
- [2] Stewart G R 1997 *Phys. Rev. B* **15** 1143
- [3] Chaumont C and Bernier J C 1983 *Solid State Commun.* **48** 357
- [4] Ozin G A 1992 *Adv. Mater.* **4** 612
- [5] Stucky G D 1992 *Prog. Inorg. Chem.* **40** 99

-
- [6] Vogel E M 1989 *J. Am. Ceram. Soc.* **72** 719
 - [7] Flytzanis C, Hache F, Klein M C, Ricar D and Rossingnol P 1991 *Prog. Opt.* **29** 321
 - [8] Cai W P and Zhang L D 1996 *J. Phys.: Condens. Matter* **8** L591
 - [9] Hayakawa T, Selvan S T and Nogami M 1999 *Appl. Phys. Lett.* **74** 1513
 - [10] Lermé J, Palpant B, Pével B, Pellarin M, Treilleux M, Vialle J L, Perez A and Broyer M 1998 *Phys. Rev. Lett.* **80** 5105
 - [11] Xie Y, Qiao Z P, Chen M, Zhu Y J and Qian Y T 1999 *Adv. Mater.* **11** 1512
 - [12] Ershov G and Henglein A 1993 *J. Phys. Chem.* **97** 3434
 - [13] Liu F X, Tang M, Liu L, Lu S, Wang J Y, Chen Z Y and Ji R 2000 *Phys. Status Solidi a* **179** 437
 - [14] Kreibig U and Vollmer M 1995 *Optical Properties of Metal Clusters* (Berlin: Springer)
 - [15] Arnold G W 1975 *J. Appl. Phys.* **46** 4466
 - [16] Ohring M 1992 *The Materials Science of Thin Films* (London: Academic)
 - [17] Smithard M A 1974 *Solid State Commun.* **14** 407
 - [18] Fedrigo S, Harbich W and Buttet J 1993 *Phys. Rev. B* **47** 10706
 - [19] Yang L, Li G H and Zhang L D 2000 *Appl. Phys. Lett.* **76** 1537
 - [20] Ferreira M P, Wander L and Vasconcelos 2000 *J. Non-Cryst. Solids* **273** 175
 - [21] Kresin V V 1995 *Phys. Rev. B* **51** 1844
 - [22] Kreibig U, Gartz M and Hilger A 1997 *Ber. Bunsenges. Phys. Chem.* **101** 1593
 - [23] Cohen R W, Cody G D, Counts M D and Abeles B 1973 *Phys. Rev. B* **8** 3689
 - [24] Tiggesbaumker J, Koller L, Broer K H M and Liebsch A 1993 *Phys. Rev. A* **48** R1749
 - [25] Kreibig U and Genzel L 1985 *Surf. Sci.* **156** 678